

Quantitative determination of contact depth during spherical indentation of metallic materials—A FEM study

Sung Hoon Kim*, Baik Woo Lee, Yeol Choi, Dongil Kwon

School of Materials Science and Engineering, Seoul National University, Seoul 151-742, South Korea

Accepted 24 August 2005

Abstract

The continuous indentation technique, because it is fast, precise and nondestructive, has been widely used to determine such mechanical properties as flow properties, residual stress, fracture properties, viscoelastic properties and hardness of materials and structural units. In particular, continuous indentation by a spherical indenter can provide hardness and flow properties, such as yield strength, tensile strength and work-hardening exponent, using the characteristic that strain from the loaded indenter changes with indentation depth. Since the stress and strain values on the flow properties are defined based on the contact area between the indenter and material in the loaded state, accurate determination of the contact area is essential. Determination of the contact area is closely connected with the pile-up/sink-in behavior.

In this study, the pile-up/sink-in phenomenon is considered as two independent behaviors, elastic deflection and plastic pile-up, which can be respectively described by a formula. The formulas can be obtained from FE simulation with conditions reflecting real indentation tests for materials used for various purposes and with a wide range of material properties. By analyzing indentation morphology from the FE simulation, the two phenomena were quantified as formulas. In particular, plastic pile-up behavior was formulated in terms of work-hardening exponent and indentation ratio.

© 2005 Elsevier B.V. All rights reserved.

Keywords: Continuous indentation; Spherical indenter; Contact depth; Elastic deflection; Plastic pile-up; Finite element analysis; Metallic materials

1. Introduction

Continuous indentation technique has been most widely used to determine many kinds of mechanical properties, such as flow properties [1,2], residual stress [3,4], fracture properties [5,6], viscoelastic properties [7,8] and hardness [9,10], because of its fast, precise and nondestructive merit. Among them, continuous indentation using a spherical indenter can provide Brinell hardness and flow properties, such as yield strength, tensile strength and work-hardening exponent, using the fact that strain from the loaded indenter changes with indentation depth. Because the stress and strain values on the flow curve are defined on the basis of the contact area between indenter and material in the loaded state, accurate contact area determination is essential to accurate stress and strain values. Determination of the contact area is closely connected with elastic deflection and the plastic pile-up behavior of the material-indenter contact region.

Early research on determining the contact area considered elastic deflection and plastic pile-up as one phenomenon, “pile-up/sink-in”, and represented it as a function of the work-hardening exponent of the indented material [11–15]. More recent work has reported that the pile-up/sink-in is related to yield strain (the ratio of yield strength Y to elastic modulus E) and indentation ratio (indentation depth h over indenter radius R) as well as to the work-hardening exponent, but did not describe the phenomenon as a formula containing these parameters [16,17]. Because the concept of pile-up/sink-in behavior includes the two phenomena “elastic deflection” and “plastic pile-up”, it is natural that more than three parameters influence the behavior, and thus, that it cannot be quantified in any one formula.

In this study, the pile-up/sink-in phenomenon is considered two independent behaviors, “elastic deflection” and “plastic pile-up”, which can be described by one formula each. The formulas can be obtained from FE simulation with the boundary conditions reflecting real indentation tests for materials with a wide range of material properties. By analyzing indentation morphology from the FE simulation, the two phenomena were quantified;

* Corresponding author. Tel.: +82 2 880 8404; fax: +82 2 886 4847.
E-mail address: iljiok@plaza.snu.ac.kr (S.H. Kim).

in particular, plastic pile-up behavior was formulated in terms of the work-hardening exponent and indentation ratio.

2. Theoretical background and modeling

2.1. Indentation load–depth curve and indentation morphology

The indentation load–depth curve, primary data obtained from the continuous indentation test, shows the load imposed on the material by the indenter and the depth to which the indenter penetrates (see Fig. 1). Several depths are defined from this curve. The *maximum depth* h_{\max} is the total displacement of the material and the indenter at *maximum load* L_{\max} , including elastic and plastic deformation. In unloading, elastic deformation is fully recovered and the initial slope of the unloading curve is the indentation stiffness of the specimen and the indenter S . Thus, the *final depth* h_f is the plastic deformation of the material.

In addition, some indentation depths are defined from the indentation morphology (see Fig. 2) at maximum load. The *contact depth* h_c is the depth of actual contact between material and indenter at maximum load. The *deflection depth* h_d is the depth

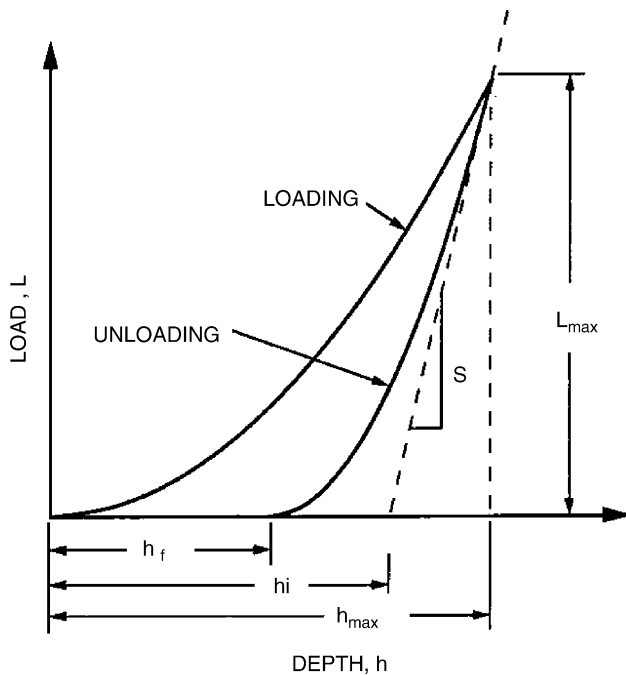


Fig. 1. Indentation load–depth curve.

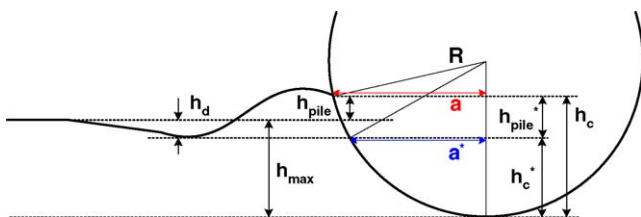


Fig. 2. Indentation morphology by spherical indenter at maximum load.

to which the maximum indentation depth h_{\max} is reduced by elastic deflection of the material, where the difference of h_{\max} and h_d is the *elastic contact depth* h_c^* . The *increase in depth* from h_c^* by the plastic pile-up phenomenon is defined as h_{pile}^* . Finally, the *real contact depth* h_c is expressed as:

$$h_c = h_{\max} + h_{\text{pile}} = h_{\max} - h_d + h_{\text{pile}}^* \quad (1)$$

2.2. Previous research on contact area

Research on determining an accurate contact area has two branches: work considering ‘elastic deflection’ and ‘plastic pile-up’ as one phenomenon, namely the ‘pile-up/sink-in’ (approach 1), and work considering them different two phenomena (approach 2). In approach 1, Norbury and Samuel suggested for the first time that pile-up/sink-in was related to the work-hardening exponent of the indented material [11]. Subsequently, Matthews [13], Hill et al. [14] and Alcalá et al. [15] described the pile-up/sink-in effect as a quantitative function of work-hardening exponent through an analysis based on FE simulation. Since these functions contain only the work-hardening exponent, they cannot describe the pile-up/sink-in behavior of materials having different material properties. For this reason, Taljat and Pharr suggested, from FE simulation assuming very simple plastic deformation behavior, that pile-up/sink-in behavior was related to Y/E and h/R as well as n , here Y/E is yield strain and R is the radius of the ball indenter [16]. However, a quantitative equation or function was not suggested in this work due to the complex relation among the properties, indentation parameters and pile-up/sink-in parameter, and the results were hard to apply to the deformation behavior of real materials due to the assumption of simple linear plastic deformation behavior.

On the other hand, in approach 2, Herbert et al. suggested determining contact area by using only the ‘elastic deflection effect’ [18]:

$$h_c \approx h_c^* = h_{\max} - h_d \quad (2)$$

$$h_d = \omega(h_{\max} - h_i) \quad (3)$$

where h_i is the intercept depth obtained by extrapolating the tangent line of the initial unloading curve to $L=0$, as shown in Fig. 1, and ω is a constant related to the geometry of the indenter; $\omega=0.72$ for a conical indenter, $\omega=0.75$ for a paraboloid of revolution and $\omega=1$ for a flat punch. However, it has been found that neglecting the ‘plastic pile-up effect’ can underestimate the true contact area by as much as 60% [19,20]. For this reason, the equation used by Herbert et al. is inadequate to determine a precise contact area, but is pertinent to determining an elastic deflection depth h_d . In the present study, h_c in Herbert et al. is called h_c^* , the elastic contact depth excluding plastic pile-up/sink-in effect. Subsequently, Ahn and Kwon [1] suggested that contact area could be determined by describing the plastic pile-up height increase from h_c^* through Hill’s equation. The work was the first suggestion that elastic deflection and plastic pile-up should be handled by individual equations or functions. However, in Ref. [1], the plastic

pile-up effect was represented as a function of only the work-hardening exponent, without consideration of the indentation ratio.

3. Simulations and experiments

Simulation of the indentation process was carried out using ABAQUS finite element code. An axisymmetric FE analysis was employed with the indenter modeled as a rigid spherical ball. A cylindrical specimen of diameter 200 mm and height 100 mm was modeled with 3738 linear four-node elements; indenter diameter was 1 mm. The indentation depth was selected as 250 μm , as in the indentation test. A cylindrical coordinate system with radial coordinate r and axial coordinate z was used. The bottom surface of the specimen has the z displacement fixed, whereas free movement is allowed in the r direction. The appropriate boundary conditions for modeling the axisymmetric behavior were applied along the centerline, and a free surface was modeled at the top and outside surface of the specimen. A friction coefficient μ of 0.2 was used in the computations to model the behavior of the indenter/specimen interface, which was determined as the optimal condition reflecting well the real indentation load–depth curve though the comparison of the result from simulation with that from continuous indentation test although the influences of friction were examined using μ of 0.1, 0.2, 0.3 and 0.5.

The basic input material properties were the true stress–true strain curves, elastic modulus and Poisson's ratio for each material shown in Table 1. Tensile properties were measured from tensile tests using the Instron 5582 according to ASTM E8-00. Elastic modulus and Poisson's ratio were measured by the ultrasonic method using Tektronics Inc.'s TDS220. And 36 imaginary materials, shows Hollomon type plastic stress–strain behavior, were made for the different conditions of n , E and Y within range of the properties for metallic materials. The variety of

material properties was covered by values of n with range from 0.05 to 0.5, Y from 100 to 800, E from 100 to 400 and ν of 0.3.

4. Results and discussion

4.1. Indentation parameters related to determining contact area

The behavior treated in previous research as pile-up/sink-in was divided in this study into two behaviors: elastic deflection and plastic pile-up. Hence, the key indentation parameters for determining an accurate contact area are the elastic deflection depth h_d and the plastic pile-up depth h_{pile}^* . As h_{pile}^* is the depth generated by plastic deformation during indenter penetration into the material, it is related to such plastic materials properties as the work-hardening exponent n and indentation ratio h/R , equivalent to the indentation strain. On the other hand, because h_d is the depth induced by elastic deflection of material during loading, it is also related to such elastic parameters as yield strain, Y/E . Because previous research had focused on the height increase from the reference plane, including both elastic deflection and plastic pile-up effects, the results for $h_{\text{pile}}/h_{\text{max}}$, were related to Y/E as well as to n and h/R . Fig. 3, the results from FE morphology, shows these relationships; $h_{\text{pile}}/h_{\text{max}}$ is the 'pile-up/sink-in parameter' in Hill's and Matthews' research. As shown in the figure, the pile-up/sink-in parameter changes with Y/E for fixed n and indentation ratio.

On the other hand, a pure plastic pile-up parameter defined as h_{pile}^*/h_c^* in this study was nearly independent of Y/E , as shown in Fig. 4. This means that plastic pile-up/sink-in behavior is the only plastic characteristic almost independent of Y/E , an elastic property; hence, the behavior can be represented as a function of n and h/R if elastic deflection and plastic pile-up/sink-in effects are separated.

Table 1
Materials used in this study

Material	Class	Yield strength [MPa]	Tensile strength [MPa]	Work-hardening exponent	Elastic modulus [GPa]	Poisson's ratio
Al2011	Aluminum alloy	270.00	474.00	0.1858	74.09	0.3355
API X42	Pipe steel	436.20	619.70	0.1440	206.52	0.2969
API X65	Pipe steel	494.72	647.39	0.1532	216.28	0.2687
KP	Pipe steel	765.50	1003.40	0.1237	211.18	0.2861
NAK	Plastic mold steel	1207.44	1358.98	0.0508	202.62	0.2868
SA508	Pressure vessel steel	638.42	960.39	0.1376	201.67	0.2957
SCM21	Structural steel	279.53	628.97	0.2057	208.83	0.2684
SCM440	Structural steel	654.07	1027.22	0.1598	210.64	0.2885
S45C	Structural steel	374.14	920.13	0.3378	209.05	0.2873
SK3	Tool steel	244.10	690.70	0.2640	208.74	0.2929
SK4	Tool steel	311.15	833.14	0.2115	209.15	0.2908
SKD11	Tool steel	242.90	932.10	0.2759	215.66	0.2942
SKD61	Tool steel	350.25	901.21	0.2910	221.48	0.2676
SKH51	Tool steel	263.85	920.13	0.2591	246.80	0.2411
SS400	Structural steel	272.70	514.36	0.2345	211.26	0.2984
SUJ2	Bearing steel	322.80	795.30	0.2442	214.85	0.2864
SUS304	Stainless steel	306.40	1076.71	0.3418	197.95	0.2901
SUS316	Stainless steel	366.65	956.93	0.2806	197.16	0.2913

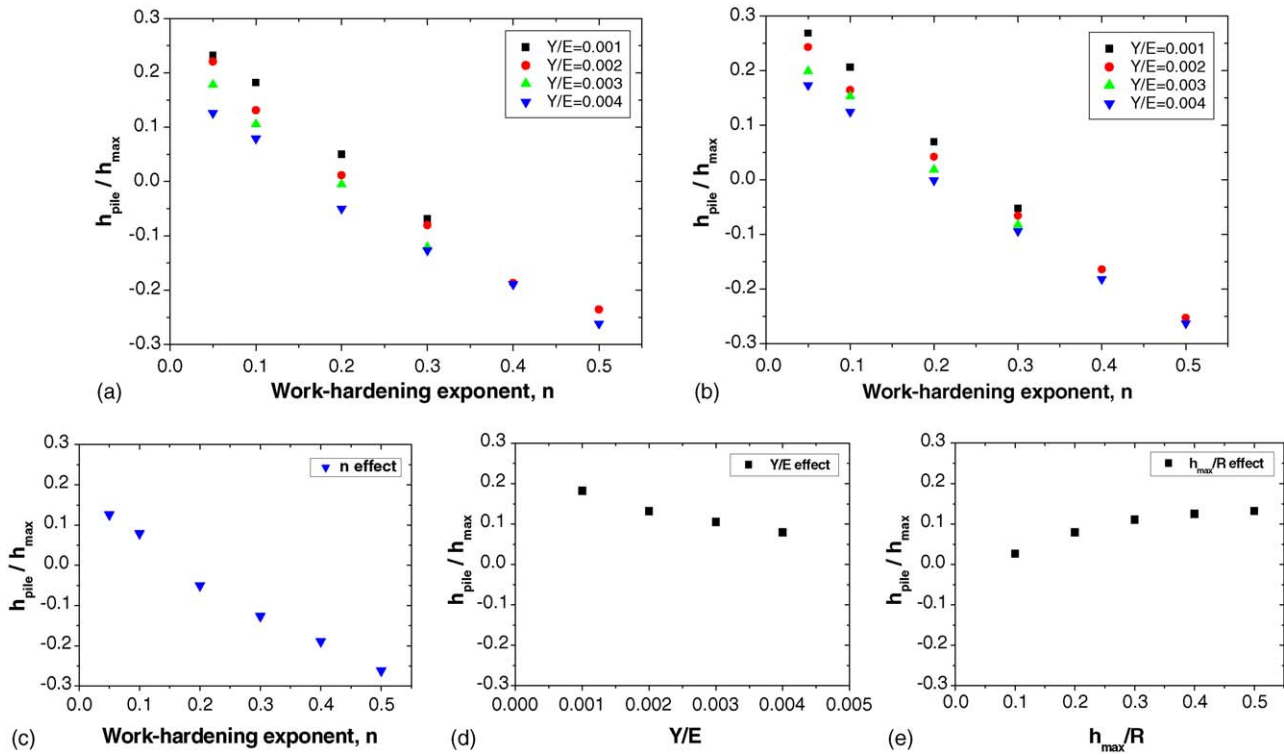


Fig. 3. Dependency of pile-up/sink-in parameter on work-hardening exponent and yield strain for: (a) $h_{max}/R = 0.2$; (b) $h_{max}/R = 0.4$; (c) $h_{max}/R = 0.2$, $Y/E = 0.004$; (d) $h_{max}/R = 0.2$, $n = 0.1$; (e) $Y/E = 0.004$, $n = 0.1$ (based on the results of imaginary material).

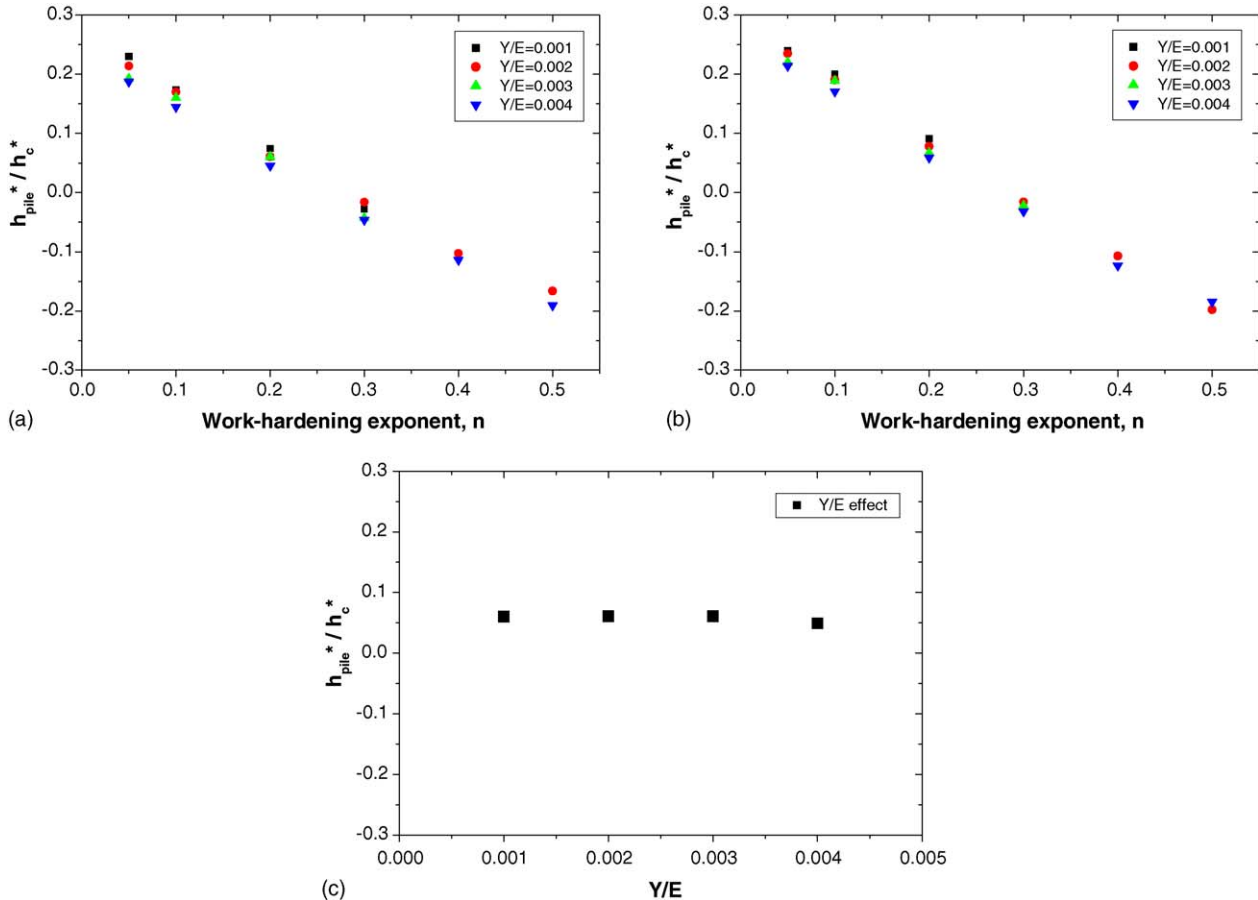


Fig. 4. Dependency of plastic pile-up/sink-in parameter on work-hardening exponent and yield strain for: (a) $h_{max}/R = 0.2$; (b) $h_{max}/R = 0.4$; (c) $h_{max}/R = 0.2$, $n = 0.2$ (based on the results of imaginary material).

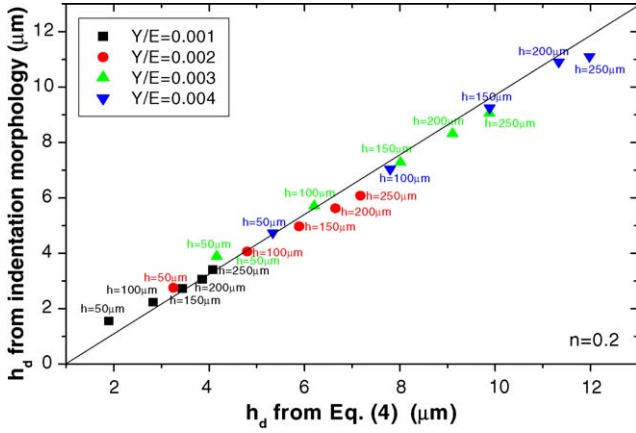


Fig. 5. Comparison of results between h_d from Eq. (4) and from indentation morphology (based on the results of imaginary material).

4.2. Determining elastic deflection depth

In this study, the deflection depth h_d was determined from indentation morphology by FE simulation. However, in an actual continuous indentation test, it would be determined from a specific equation by using indentation parameters from the indentation load–depth curve. Doerner and Nix’s or Oliver and Pharr’s equation, Eq. (4), was mostly used as the specific equation. To verify the equation, the deflection depth determined by analyzing the indentation load–depth curve by FE simulation based on the equation was compared to the deflection depth derived from indentation morphology by FE simulation.

Fig. 5 compares the deflection depth results for materials having work-hardening exponent 0.2 and different Y/E values. The results of Eq. (4) accord well with that from morphology with an error range smaller than 5%; thus, this equation is good enough to describe elastic deflection depth. In addition, the increase of h_d with Y/E indicates that elastic deflection depth depends only on Y/E because it is an elastic characteristic that is recovered after unloading. The elastic deflection depth can be calculated from Eq. (4) and the equation can be

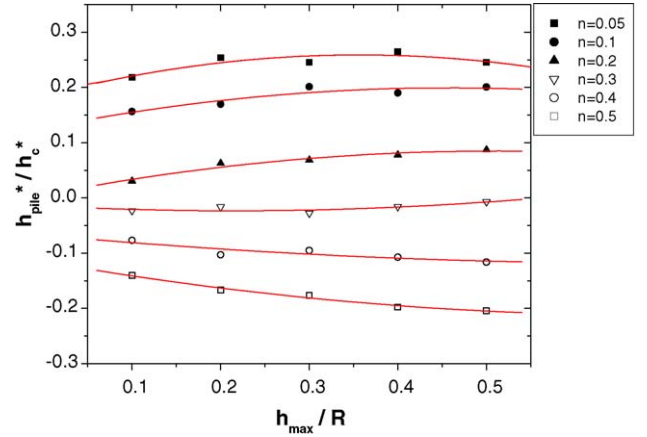


Fig. 6. Plastic pile-up parameter as the function of h_{max}/R (based on the results of imaginary material).

converted to:

$$h_d = \omega \frac{L_{max}}{S_i}, \quad (4)$$

where S_i , the experimentally measured stiffness of the upper portion of the unloading data, is related to the reduced modulus E_r :

$$S_i = \frac{2}{\sqrt{\pi}} E_r \sqrt{A_c}. \quad (5)$$

Here

$$\frac{1}{E_r} = \frac{1 - \nu^2}{E} + \frac{1 - \nu_i^2}{E_i}, \quad (6)$$

where E and ν are elastic modulus and Poisson’s ratio for the specimen and E_i and ν_i are the same parameters for the indenter. Since elastic deflection depth is related to S , it is an elastic property; as stated above, h_d is dependent on Y/E .

4.3. Determining plastic pile-up depth considering indentation ratio

The plastic pile-up parameter h_{pile}^*/h_c^* has an almost linear relation with the work-hardening exponent at fixed indentation

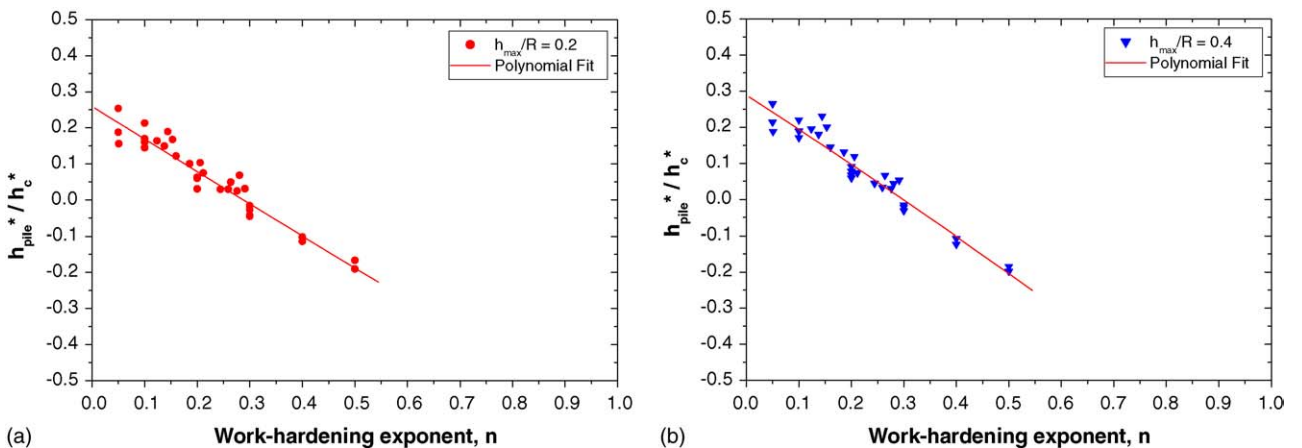


Fig. 7. First step of functionalization; polynomial fitting for the fixed h_{max}/R .

Table 2
Determined constants of Eq. (9)

h_{\max}/R	α	b_1	b_2
0.1	0.2002	-3.4414	0.1098
0.2	0.2592	-3.4234	0.0798
0.3	0.2835	-3.4242	0.0584
0.4	0.2889	-3.4016	0.0710
0.5	0.2867	-3.4221	0.0615

ratio, as shown in Fig. 4(a). On the other hand, for different h_{\max}/R , the plastic pile-up parameter has a quadratic relation with h_{\max}/R , as shown in Fig. 6. To reflect the dependence of the plastic pile-up parameter on both n and h_{\max}/R , a second-order bivariate dependency is introduced:

$$\frac{h_{\text{pile}}^*}{h_c^*} = a(1 + b_1n + b_2n^2) \left(1 + c_1 \frac{h_{\max}}{R} + c_2 \left(\frac{h_{\max}}{R} \right)^2 \right), \quad (7)$$

where a , b_1 , b_2 , c_1 and c_2 are constants.

The function describing the plastic pile-up effect is determined in two steps. First, a term of the work-hardening exponent is formulated as Eq. (8) for fixed h_{\max}/R values. Second, a variable α is represented as a function of h_{\max}/R :

$$\frac{h_{\text{pile}}^*}{h_c^*} = \alpha(1 + b_1n + b_2n^2), \quad (8)$$

where

$$\alpha = a \left(1 + c_1 \frac{h_{\max}}{R} + c_2 \left(\frac{h_{\max}}{R} \right)^2 \right) \quad (9)$$

In the first step, fitting results are shown in Fig. 7 as procedures to determine a function of n . Even though the term for n was initially taken as second-order, the fitting results were nearly linear for n . The constants determined from fitting (see Table 2) show that the term for the work-hardening exponent is nearly first-order linear due to the very small constant b_2 . This result is similar to McClintock's linear relationship between the pile-up parameter and work-hardening exponent [12]. The b_1 and b_2 values for different α values, meaning different h_{\max}/R values, are nearly constant, showing the independency between two terms and the validity of the function shape.

The variable α changes with h_{\max}/R as shown in Fig. 8, and therefore, can be fitted as a second-order term for h_{\max}/R . The function for plastic pile-up/sink-in can now be expressed by a second-order bivariate:

$$\frac{h_{\text{pile}}^*}{h_c^*} = 0.131(1 - 3.423n + 0.079n^2) \times \left(1 + 6.258 \frac{h_{\max}}{R} - 8.072 \left(\frac{h_{\max}}{R} \right)^2 \right) \quad (10)$$

To show the validity of Eq. (10), the results of the plastic pile-up parameter h_{pile}^*/h_c^* from the equation are compared in Fig. 9 with those from indentation morphology in FE simulation. Agreement is good for materials having different work-hardening exponent and indentation ratio.

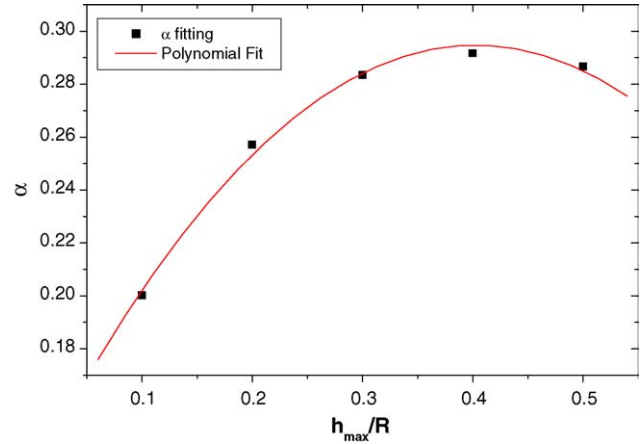


Fig. 8. Determination of α as the function of h_{\max}/R .

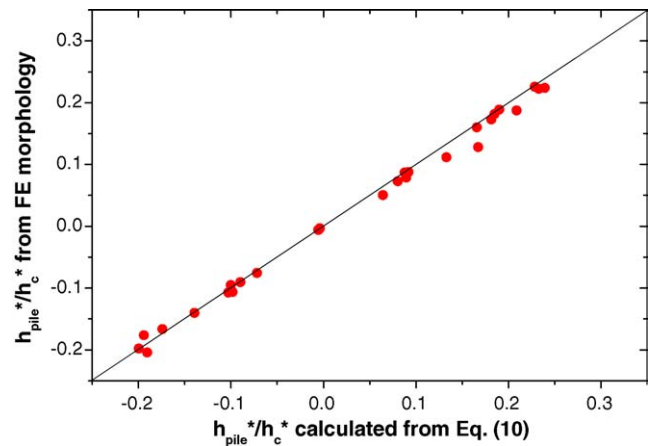


Fig. 9. Comparison of the results between h_{pile}^*/h_c^* from the function in this study and from FE morphology.

5. Conclusions

Previous research regarded the pile-up/sink-in effect as one phenomenon including elastic deflection and plastic pile-up and tried to find the relationship between it and various material properties or indentation parameters. The present study used FE simulation for real and imaginary materials to reconfirm that the pile-up parameter h_{pile}/h_{\max} in this previous research has a complex relationship with n , Y/E and h_{\max}/R . We, therefore, divided the pile-up/sink-in phenomenon into two phenomena, elastic deflection and plastic pile-up, which could be described by two equations.

Elastic deflection is well explained by the equation suggested by Oliver and Pharr [9], on the basis of the results from this equation and from indentation morphology by FE simulation. Plastic pile-up, excluding elastic deflection, was related to n and h_{\max}/R but not to Y/E ; by analyzing the relationships among indentation morphology, input properties and indentation parameters, the plastic pile-up was represented as a formula of second-order bivariate shape for n and h_{\max}/R . The plastic pile-up parameter from this formula agreed well with that from indentation morphology by FE simulation, showing that the

plastic pile-up/sink-in phenomenon is explained well as the function of only two parameters, n and h_{\max}/R .

References

- [1] J.H. Ahn, D. Kwon, *J. Mater. Res.* 16 (2001) 3170.
- [2] F.M. Haggag, ASTM STP 1204, Philadelphia, 1993, p. 27.
- [3] S. Suresh, A.E. Giannakopoulos, *Acta Mater.* 46 (1998) 5755.
- [4] Y.H. Lee, D. Kwon, *J. Mater. Res.* 17 (2002) 901.
- [5] J. Malzbender, G. de With, *Surf. Technol.* 135 (2000) 60.
- [6] K.L. Murty, M.D. Mathew, Y. Wang, V.N. Shah, F.M. Haggag, *J. Pressure Vessels Piping* 75 (1998) 831.
- [7] S.A.S. Asif, K.J. Wahl, R.J. Colton, *Rev. Sci. Inst.* 70 (1999) 2408.
- [8] B.N. Lucas, W.C. Oliver, J.E. Swindeman, *Mater. Res. Soc. Symp. Proc.* 522 (1998) 3.
- [9] W.C. Oliver, G.M. Pharr, *J. Mater. Res.* 7 (1992) 1564.
- [10] S.H. Kim, E.C. Jeon, D. Kwon, *J. Eng. Mater. Technol.* 127 (2005) 154.
- [11] A.L. Norbury, T. Samuel, *J. Iron Steel Inst.* 117 (1928) 673.
- [12] S.S. Rhee, F.A. McClintock, *Proceedings of the Fourth US National Conference on Applied Mechanics*, ASME, Berkeley, California, 1962.
- [13] J.R. Matthews, *Acta Metall.* 28 (1980) 311.
- [14] R. Hill, B. Storkers, A.B. Zdunek, *Proc. R. Soc. Lond.* A423 (1989) 301.
- [15] J. Alcalá, A.C. Barone, M. Anglada, *Acta Mater.* 48 (2000) 3451.
- [16] B. Taljat, G.M. Pharr, *Mater. Res. Soc. Symp. Proc.* 522 (1998) 33.
- [17] Y.T. Cheng, C.M. Cheng, *Philos. Mag. A* 78 (1998) 115.
- [18] E.G. Herbert, G.M. Pharr, W.C. Oliver, B.N. Lucas, J.L. Hay, *Thin Solid Films* 398–399 (2001) 331.
- [19] Y.Y. Lim, M.M. Chaudhri, Y. Enomoto, *J. Mater. Res.* 14 (1999) 2134.
- [20] A. Bolshakov, G.M. Pharr, *J. Mater. Res.* 13 (1998) 1049.